AUTHOR QUERY FORM

ELSEVIER	**Journal: POLY** **Article Number: 10405**	**Please e-mail or fax your responses and any corrections to:** **E-mail: corrections.esch@elsevier.sps.co.in** **Fax: +31 2048 52799**

Dear Author,

Please check your proof carefully and mark all corrections at the appropriate place in the proof (e.g., by using on-screen annotation in the PDF file) or compile them in a separate list. Note: if you opt to annotate the file with software other than Adobe Reader then please also highlight the appropriate place in the PDF file. To ensure fast publication of your paper please return your corrections within 48 hours.

For correction or revision of any artwork, please consult http://www.elsevier.com/artworkinstructions.

Any queries or remarks that have arisen during the processing of your manuscript are listed below and highlighted by flags in the proof. Click on the 'Q' link to go to the location in the proof.

Location in article	Query / Remark: click on the Q link to go Please insert your reply or correction at the corresponding line in the proof
Q1	Please confirm that given name(s) and surname(s) have been identified correctly.
Q2	Please check the telephone/fax number of the corresponding author, and correct if necessary.
Q3	Please provide the significance of symbol '∗' in Table 2.

Please check this box if you have no corrections to make to the PDF file ☐

Thank you for your assistance.

Allen Bowden, Simon J. Coles, Mateusz B. Pitak, Andrew W.G. Platt

Polyhedron xx (2013) xx

Complexes of lanthanide nitrates with tri-isopropylphosphine oxide

The structures of lanthanide nitrate complexes of tri-isopropylphosphine oxide vary with the size of the lanthanide ion. Lighter lanthanides form 9 coordinate structures, erbium an ionic 8-coordinate cation and ytterbium and lutetium 8-coordinate complexes with a pseudo hexagonal bipyramidal geometry.

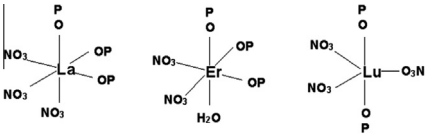

Polyhedron xxx (2013) xxx–xxx

Contents lists available at ScienceDirect

Polyhedron

journal homepage: www.elsevier.com/locate/poly

Complexes of lanthanide nitrates with tri-isopropylphosphine oxide

Allen Bowden [a], Simon J. Coles [b], Mateusz B. Pitak [b], Andrew W.G. Platt [c,*]

[a] Department of Chemistry and Analytical Sciences, The Open University, Walton Hall, Milton Keynes, MK7 6BT, UK
[b] UK National Crystallography Service, Chemistry, Faculty of Natural and Environmental Sciences, University of Southampton, Highfield Campus, Southampton SO17 1BJ, UK
[c] School of Science, Staffordshire University, Leek Road, Stoke-on-Trent ST4 2DF, UK

ARTICLE INFO

Article history:
Received 19 August 2013
Accepted 27 October 2013
Available online xxxx

Keywords:
Lanthanide nitrate
Phosphine oxide
Crystal structure
NMR spectroscopy

ABSTRACT

The complexes formed on reaction of tri-isopropylphosphine oxide ($(C_3H_7)_3PO$ = L) and lanthanide nitrates have been studied. The new compounds have been characterised by elemental analysis, infrared and ^{31}P NMR spectroscopy in CD_2Cl_2 solution. On reaction of lanthanide nitrates and L in 1:3 ratios, well defined $Ln(NO_3)_3L_3$ are obtained for Ln = La–Eu with complexes for the heavier lanthanides forming mixtures of $Ln(NO_3)_3L_3$ and $Ln(NO_3)_3L_2$. Analytically pure complexes $Ln(NO_3)_3L_2$ can be isolated for Yb and Lu. Single crystal X-ray structures for $Ln(NO_3)_3L_3$, Ln = La (**1**), Ce (**2**), Pr (**3**), the ionic complex $[Er(NO_3)_2L_3(H_2O)][NO_3]$ (**4**) and $Ln(NO_3)_3L_2$, Ln = Yb (**5**), Lu (**6**) are reported. The ^{31}P solution NMR spectra of $Ln(NO_3)_3L_3$ show that the complexes are fluxional at ambient temperature with spectra consistent with static structures observed at lower temperatures for some complexes. The structures and solution properties are discussed in terms of the steric and electronic properties of the ligand.

1. Introduction

Complexes of lanthanide nitrates with phosphine oxides have been investigated since the 1960s. The majority of studies have centred on triphenylphosphine oxide [1–4] with relatively little attention given to trialkylphosphine oxides. $Nd(NO_3)_3(R_3PO)_3$ (R = Me, Et) [5] were characterised by elemental analysis, infrared and electronic spectroscopy and the isolation of complexes $Ln(NO_3)_3(R_3PO)_3$ (R = butyl, octyl) show that the 3:1 ligand to metal ratio is common [6] in these systems. The same composition has been deduced for $Am(NO_3)_3(R_3PO)_3$ and $Cm(NO_3)_3(R_3PO)_3$ in the solvent extraction studies with Bu_3PO and Oct_3PO [7]. Mixed trialkylphosphine oxides $RR'R''_3PO$ (R, R′, R″ = hexyl, heptyl and octyl) have been used as extractants for lanthanide ions either alone [8,9] or in synergy with alkylphosphinic acids [10].

We have previously examined the formation and properties of lanthanide nitrate complexes with R_3PO with varying steric demands. With Et_3PO as ligand complexes $Ln(NO_3)_3(Et_3PO)_3$ form for the lighter lanthanides and mixtures of $Ln(NO_3)_3(Et_3PO)_3$ and $Ln(NO_3)_3(Et_3PO)_2$ for the heavier metals [11]. On increasing the size of the ligand with R = cyclohexyl [12] and $^iBu_3PO$ [13] we find that $Ln(NO_3)_3(R_3PO)_3$ form throughout the lanthanide series, with subtle variations in structure as the ionic radius decreases. When R = ^{t}butyl the greater steric effects mean that only $Ln(NO_3)_3(^tBu_3PO)_2$ are formed for all Ln, again with subtle differences in the structures as the series is traversed [14]. The balance between increasing steric effects and increasing basicity of the phosphine oxide [15], can be seen to be responsible for the changes in composition. Thus for Et_3PO pure $Ln(NO_3)_3L_3$ cannot be obtained for heavier lanthanides in contrast to the situation with the larger but more basic Cy_3PO and $^iBu_3PO$ where the increased basicity dominates steric effects and $Ln(NO_3)_3L_3$ can be isolated for all Ln. In this paper, we report our findings on complexes of $^iPr_3PO$ = L which has intermediate steric demands based on the cone angles (θ) of the parent phosphines. For $^iPr_3P$ $\theta = 160°$ whilst Et_3P has $\theta = 132°$ and $^tBu_3P$ has $\theta = 182°$ [16] and we felt it of interest to investigate the influence this might have on the structures and properties of the resultant complexes.

2. Results and discussion

The reactions of lanthanide nitrates with L in hot ethanol afforded solid complexes on cooling the reaction mixtures Ln = La–Er, or on cooling ethanol/diethyl ether solutions for Ln = Yb, Lu. Elemental analyses indicate that $Ln(NO_3)_3L_3$ form for Ln = La–Eu. The bulk material isolated from the reaction with $Er(NO_3)_3$ and L analysed as a mixture of 1:3 and 1:2 complexes, similar to the behaviour of the Et_3PO complexes with the heavier lanthanides [13]. Similarly, attempted preparation of analogous complexes for Ln = Yb and Lu gave complexes which on the basis of ^{31}P NMR spectroscopy (discussed below) do not correspond to the expected 1:3 complexes or any other simple composition. On carrying out the reaction with a 1:2 ratio complexes were obtained which analysed well for $Ln(NO_3)_3L_2$, Ln = Yb, Lu. Attempted preparation of $Nd(NO_3)_3L_2$ by the same method led to the isolation of material

* Corresponding author. Tel.: +44 1782 294784; fax: +44 1782 745506.
E-mail address: a.platt@staffs.ac.uk (A.W.G. Platt).

0277-5387/$ - see front matter © 2013 Published by Elsevier Ltd.
http://dx.doi.org/10.1016/j.poly.2013.10.028

with an identical infrared spectrum to that of the fully characterised $Nd(NO_3)_3L_3$ complex.

The electrospray mass spectra of the complexes were obtained from CH_2Cl_2/CH_3CN and show the $[M–NO_3]^+$ ion as the most abundant ion in the positive ion mode for all complexes. That this is also the case for $Ln(NO_3)_3L_2$ (Ln = Yb, Lu) implies that $[Ln(NO_3)_2L_3]^+$ is particularly stable in the gas phase. The electrospray process leads to ligand redistribution and further ionisation as we have noted previously with similar systems. The formation of higher coordination numbers seems restricted to the larger lanthanide ions as would be expected on steric grounds, and $[Ln(NO_3)_2L_4]^+$ is not observed beyond Nd. Full details of the spectra are given in Table S2 as supplementary information.

The infrared spectra are as expected for lanthanide nitrate complexes with phosphine oxides indicating the presence of bidentate nitrates. The positions of the absorptions show only weak trends within the series of complexes studied. For the nitrate ligands the ν_1 and ν_3 bands at 1301–1282 cm^{-1} and 1490–1440 cm^{-1}, respectively show no trend with the metal, whilst ν_4 shows a small decrease from 820 (La) to 816 cm^{-1} (Lu) and ν_5 increases from 733 (La) to 748 cm^{-1} (Lu). The spectra show subtle differences between the lighter and heavier lanthanides. For instance the ν_1 band which is split for La to Sm appears as a single band for Er–Lu.

The PO stretch is at lower wavenumber than the free ligand for which ν_{PO} = 1132 cm^{-1} and shows a small increase from La (1090 cm^{-1}) to Lu (1100 cm^{-1}) Full details of the N–O and P–O bands are shown in the supplementary information in Table S1.

The single crystal X-ray structures have been determined for $Ln(NO_3)_3L_3$, Ln = La (**1**), Ce (**2**), Pr (**3**); $[Ln(NO_3)_2(H_2O)L_3][NO_3]$, Ln = Er (**4**) and $Ln(NO_3)_3L_2$, Ln = Yb (**5**), Lu (**6**). Crystallography summary for crystal structures **1**–**6** are given in Table 1 and selected bond distances in Tables 2 and 3.

Nine coordinate neutral complexes $Ln(NO_3)_3L_3$ form with the lighter lanthanides.

These have three bidentate nitrates and three monodentate phosphine oxides and can be considered as distorted *mer*-octahedra if the nitrates are considered as pseudo-monodentate ligands bonded via the nitrogen atom as found for similar complexes of lanthanide nitrates with phosphine oxides [17]. The structure of the Ce complex is shown in Fig. 1 as a representative example. The geometry of the eight-coordinate ionic complex $[Er(NO_3)_2L_3(H_2O)]^+NO_3^-$ can similarly be considered as a distorted pseudo-

Table 1
X-ray crystallography summary for compounds **1**–**6**.

	1	**2**	**3**	**4**	**5**	**6**
Empirical formula	$C_{27}H_{63}N_3O_{12}P_3La$	$C_{27}H_{63}N_3O_{12}P_3Ce$	$C_{27}H_{63}N_3O_{12}P_3Pr$	$C_{27}H_{63}N_3O_{13}P_3Er$	$C_{18}H_{42}N_3O_{11}P_2Yb$	$C_{18}H_{42}N_3O_{11}P_2Lu$
Formula weight	853.62	854.83	855.62	897.97	711.15	713.12
Temperature (K)	120(2)	120(2)	120(2)	120(2)	100(2)	100(2)
Wavelength (Å)	0.71073	0.71073	0.71073	0.71073	0.71073	0.71073
Crystal system	tetragonal	tetragonal	tetragonal	monoclinic	orthorhombic	orthorhombic
Space group	$P4_2/n$	$P4_2/n$	$P4_2/n$	$P2_1/n$	*Pmmn*	*Pmmn*
Unit cell dimensions						
a (Å)	26.9394(6)	26.9639(7)	26.8750(4)	14.5881(12)	15.207(5)	15.198(3)
b (Å)	26.9394(6)	26.9639(7)	26.8750(4)	23.8759(15)	15.332(5)	15.338(3)
c (Å)	10.9703(3)	10.9785(3)	10.9525(2)	14.8058(11)	12.497(4)	12.487(3)
α (°)	90	90	90		90	90
β (°)	90	90	90	111.070(3)	90	90
γ (°)	90	90	90		90	90
Volume ($Å^3$)	7961.5(3)	7981.9(4)	7910.6(2)	4812.1(6)	2913.7(16)	2910.8(11)
Z	8	8	8	4	4	4
D_{calc} ($Mg\ m^{-3}$)	1.424	1.423	1.437	1.239	1.621	1.627
Absorption coefficient (mm^{-1})	1.249	1.316	1.409	1.892	3.373	3.555
F(000)	3552	3560	3568	1852	1436	1440
Crystal	rod; colourless	needle; colourless	needle; light green	lath; light pink	block; Colourless	plate; colourless
Crystal size (mm^3)	0.23 × 0.03 × 0.02	0.64 × 0.08 × 0.05	0.23 × 0.03 × 0.02	0.20 × 0.05 × 0.02	0.09 × 0.08 × 0.04	0.05 × 0.04 × 0.01
θ range for data collection (°)	2.93–27.50	2.93–25.00	3.03–27.50	2.91–25.00	2.98–27.48	2.98–27.49
Index ranges	$-34 \leqslant h \leqslant 25$, $-34 \leqslant k \leqslant 34$, $-14 \leqslant l \leqslant 12$	$-32 \leqslant h \leqslant 31$, $-27 \leqslant k \leqslant 32$, $-8 \leqslant l \leqslant 13$	$-31 \leqslant h \leqslant 34$, $-34 \leqslant k \leqslant 34$, $-14 \leqslant l \leqslant 14$	$-17 \leqslant h \leqslant 16$, $0 \leqslant k \leqslant 28$, $0 \leqslant l \leqslant 17$	$-19 \leqslant h \leqslant 19$, $-16 \leqslant k \leqslant 19$, $-16 \leqslant l \leqslant 15$	$-19 \leqslant h \leqslant 19$, $-19 \leqslant k \leqslant 19$, $-16 \leqslant l \leqslant 16$
Reflections collected	36955	37079	54074	8471	16187	66121
Independent reflections (R_{int})	9119 [0.0623]	7006 [0.1144]	9060 [0.0867]	8471 [0.0000]*	3573 [0.0225]	3576 [0.0761]
Completeness to θ = 27.50°	99.70%	99.60%	99.70%	99.80%	99.4%	99.5%
Maximum and minimum transmission	0.9755 and 0.7621	0.9371 and 0.4864	0.9724 and 0.7377	0.9631 and 0.7034	0.8769 and 0.7511	0.9653 and 0.8423
Data/restraints/parameters	9119/0/433	7006/0/433	9060/0/433	8471/0/442	3573/205/255	3576/205/255
Goodness-of-fit (GOF) on F^2	1.163	1.018	1.184	0.976	1.141	1.260
Final *R* indices [$F^2 > 2\sigma(F^2)$]	R_1 = 0.0522, wR_2 = 0.0969	R_1 = 0.0508, wR_2 = 0.0986	R_1 = 0.0644, wR_2 = 0.1121	R_1 = 0.0964, wR_2 = 0.2217	R_1 = 0.0268, wR_2 = 0.0494	R_1 = 0.0558, wR_2 = 0.1062
R indices (all data)	R_1 = 0.0741, wR_2 = 0.1077	R_1 = 0.0937, wR_2 = 0.1137	R_1 = 0.0972, wR_2 = 0.1274	R_1 = 0.1862, wR_2 = 0.2504	R_1 = 0.0300, wR_2 = 0.0508	R_1 = 0.0600, wR_2 = 0.1085
Largest difference in peak and hole (e $Å^{-3}$)	0.539 and −0.499	0.580 and −0.598	0.621 and −0.659	1.329 and −1.030	0.735 and −0.502	2.111 and −1.342

* Platon/Squeeze routine was used.

Please cite this article in press as: A. Bowden et al., Polyhedron (2013), http://dx.doi.org/10.1016/j.poly.2013.10.028

Table 2
Q3 Selected bond distances (Å) in $Ln(NO_3)_3L_3$ (Ln = La, Ce, Pr) and $[Er(NO_3)L_3(H_2O)][NO_3]$.

		La	Ce	Pr	Er			La	Ce	Pr	Er
Ln–O(N)	O11–Ln1	2.658(3)	2.649(4)	2.622(4)	2.448(10)	N–O(Ln)	N11–O11	1.258(5)	1.266(6)	1.258(6)	1.250(14)
	O12–Ln1	2.620(3)	2.606(4)	2.572(4)	2.452(8)		N11–O12	1.272(5)	1.276(6)	1.261(6)	1.252(14)
	O21–Ln1	2.621(3)	2.606(4)	2.575(4)	2.444(10)		N21–O21	1.265(5)	1.268(5)	1.269(6)	1.300(15)
	O22–Ln1	2.644(3)	2.621(4)	2.600(4)	2.435(10)		N21–O22	1.275(5)	1.270(6)	1.270(6)	1.336(15)
	O31–Ln1	2.610(3)	2.619(4)	2.600(4)			N31–O31	1.274(5)	1.279(6)	1.271(6)	1.22(2)*
	O32–Ln1	2.642(3)	2.592(4)	2.572(4)			N31–O32	1.265(5)	1.263(6)	1.269(6)	1.25(3)*
Ln–O(H_2O)					2.325(9)						
Ln–O(P)	O1–Ln1	2.398(3)	2.373(3)	2.351(4)	2.229(9)	N–O	N11–O13	1.221(5)	1.216(6)	1.228(6)	1.227(14)
	O2–Ln1	2.453(3)	2.435(3)	2.410(4)	2.207(8)		N21–O23	1.216(5)	1.222(5)	1.222(6)	1.192(15)
	O3–Ln1	2.404(3)	2.391(3)	2.371(4)	2.244(8)		N31–O33	1.221(5)	1.231(6)	1.224(7)	1.19(3)*
P–O	O1–P1	1.512(3)	1.521(4)	1.515(4)	1.528(9)						
	O2–P2	1.510(3)	1.515(4)	1.516(4)	1.531(9)						
	O3–P3	1.512(3)	1.511(4)	1.512(4)	1.497(9)						

Table 3
Selected bond distances (Å) in $Ln(NO_3)_3L_2$.

		Yb	Lu			Yb	Lu
Ln–O(N)	O2–Ln1	2.395(3)	2.358(5)	N–O(Ln)	N1–O2	1.279(4)	1.276(9)
	O3–Ln1	2.399(3)	2.391(6)		N1–O3	1.274(4)	1.266(8)
	O5–Ln1	2.422(3)	2.396(5)		N2–O5	1.274(3)	1.269(6)
	O8–Ln2	2.400(3)	2.375(6)		N3–O8	1.272(4)	1.266(8)
	O9–Ln2	2.402(3)	2.390(5)		N3–O9	1.272(4)	1.268(8)
	O11–Ln2	2.402(3)	2.382(5)		N4–O11	1.279(6)	1.259(7)
Ln–O(P)	O1–Ln1	2.156(3)	2.147(5)	N–O	N1–O4	1.210(4)	1.214(9)
	O7–Ln2	2.146(2)	2.143(5)		N2–O6	1.213(5)	1.229(11)
					N3–O10	1.214(4)	1.220(9)
P–O	O1–P1	1.510(3)	1.513(6)		N4–O12	1.212(6)	1.214(12)
	O7–P2	1.518(2)	1.514(5)				

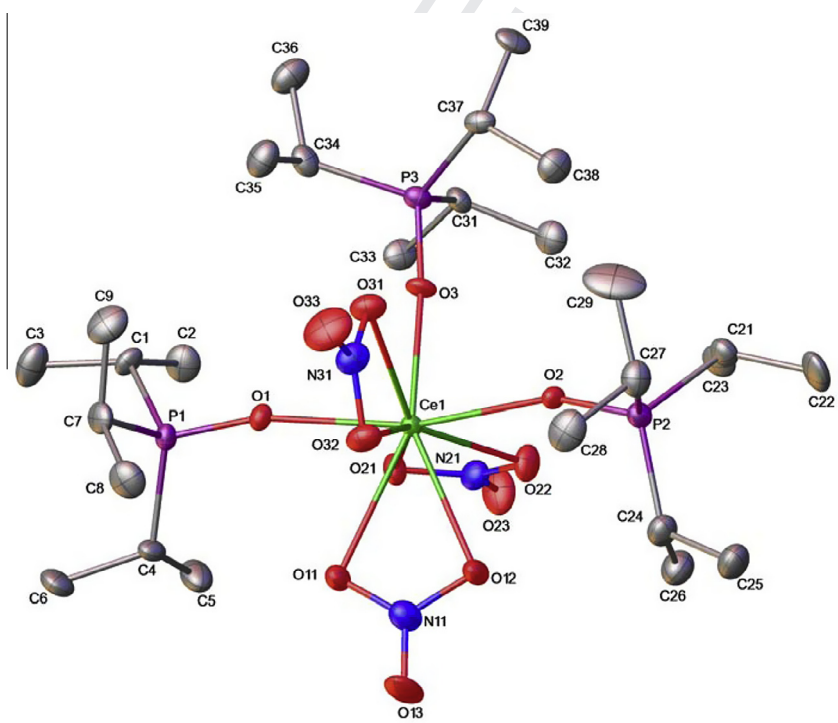

Fig. 1. The X-ray crystal structure of Ce(NO3)3L3 (2) 0. Thermal ellipsoids are drawn at 50% probability level. All hydrogen atoms are ommited for clarity.

mer octahedron with the coordinated water molecule occupying a site *trans* to a phosphine oxide and its structure is shown in Fig. 2. The elemental analysis of the bulk material does not correspond to the crystal structure and it seems likely that the crystal selected for analysis is not representative of the sample as a whole.

The Ln–O(N) and Ln–O(P) distances show the expected decrease with ionic radius of the metal. When these distances are corrected for the effect of the lanthanide contraction by subtracting the appropriate ionic radii, there are no significant differences (as tested by single factor ANOVA at 95% confidence level) between

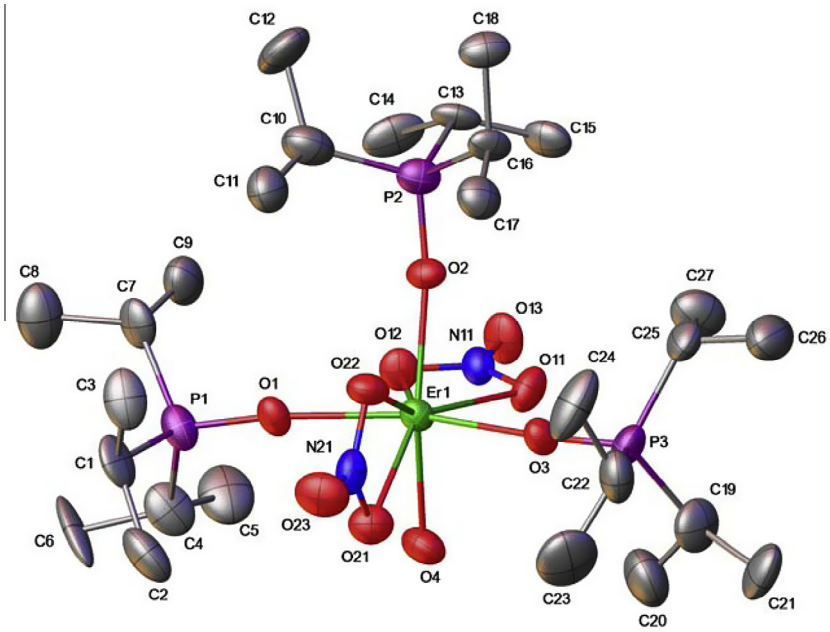

Fig. 2. The X-ray crystal structure of $[Er(NO_3)_2L_3)H_2O][NO_3]$ (4). Thermal ellipsoids are drawn at 50% probability level. All hydrogen atoms and one counterion (NO_3^{2-}) are ommited for clarity.

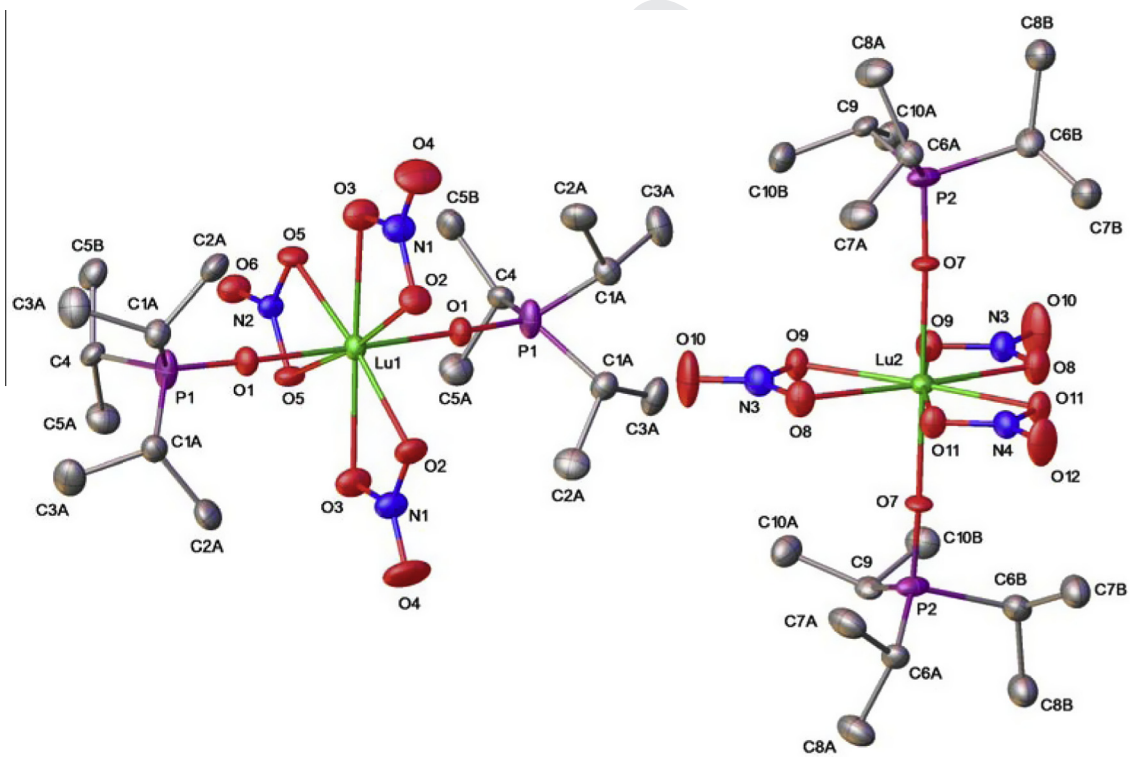

Fig. 3. The X-ray crystal structure of $Lu(NO_3)_3L_2$ (6). Displacement ellispoids −50% probability. Only one component of disorder present in the crystal structure is shown. All hydrogen atoms are omitted for clarity.

the metals. Thus the decrease can be explained as being solely due to the lanthanide contraction as we have observed in similar complexes [13,14]. The change in geometry from nine to eight-coordination can be seen as a "classic" effect of the lanthanide contraction with the loss of a nitrate from the primary coordination sphere and its replacement by the smaller water molecule. Similarly, the formation of $Ln(NO_3)L_2$ for heavier lanthanides can be explained by the lanthanide contraction.

The complexes $Ln(NO_3)_3L_2$, Ln = Yb and Lu, are isostructural with two independent molecules in the unit cell. These are 8-coordinate with a hexagonal bipyramidal geometry about the metal with the equatorial plane defined by three bidentate nitrates

and the phosphine oxides occupying the axial positions. The structure of the Lu complex is shown in Fig. 3. The structures have the same molecular geometry as one of the isomers observed for $Ln(NO_3)_3(^tBu_3PO)_2$ with the heavier lanthanides [14] and are presumably formed as a result of the increasing steric congestion around the smaller Yb and Lu ions compared with the lighter lanthanides which form $Ln(NO_3)_3L_3$. The Lu–O(N) distances are marginally shorter for the isopropyl complexes compared to the tert-butyl analogue with average Lu–O(N) distances of 2.382 Å (^iPr) and 2.392 Å (^tBu).

The $Ln(NO_3)_3L_3$ structures all have short contacts between some of the hydrogen atoms of the isopropyl groups and the coordinated oxygen atoms of the nitrate groups. The H. . .O distances are significantly shorter than the sum of the Van der Waals radii for O and H (2.61 Å). The weak H-bonded interactions are shown in Fig. 4 for the La complex and similar interactions are evident in the Ce and Pr structures. Selected distances are given in Table 4.

The strongest interactions occur between the oxygen and one of the methine protons with H. . .O distances in the region of 2.3 Å. Weaker interactions are present between methyl protons and nitrate oxygen atoms with H. . .O distances which are only slightly shorter than the sum of Van der Waals radii at just below 2.6 Å. The relative strength of the hydrogen bonding seems reasonable as the C–H proton is closer to the metal, will experience a greater inductive effect and thus have a larger residual positive charge. The hydrogen bonded distances tend to decrease from La to Pr indicating and increased strength of interaction. This could be due to an inductive effect increasing as the charge density on the lanthanide ion increases.

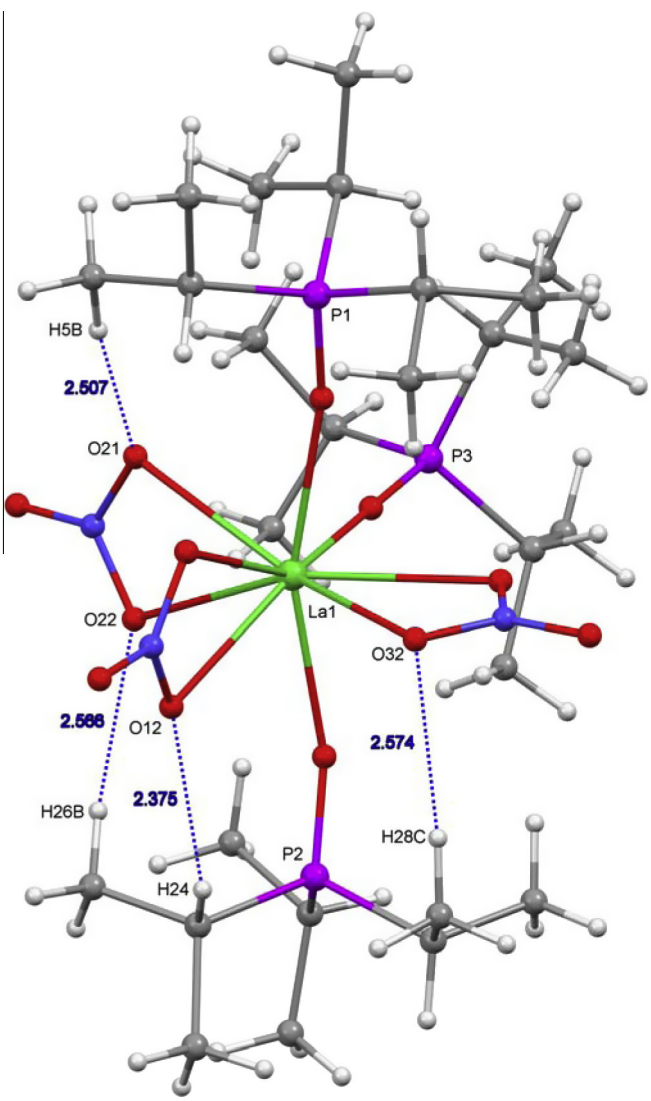

Fig. 4. The weak intermolecular C–H. . .O hydrogen bonding in $La(NO_3)_3L_3$.

Table 4
The weak hydrogen bond distances (Å) in $Ln(NO_3)_3L_3$.

	C–H. . .O [Å]		CH_3. . .O [Å]		
	O12. . .H24	O11. . .H4	O21. . .H5B	O22. . .H26B	O32. . .H28C
La	2.375	2.599	2.507	2.566	2.574
Ce	2.365	2.564	2.503	2.557	2.579
Pr	2.356	2.561	2.466	2.539	2.567

There are similar, but less extensive interactions between the methyl protons and coordinated and ionic nitrate in the Er structure. Interestingly, there are no short contacts between the methine protons and any of the coordinated nitrate oxygen atoms. The ionic nitrate has weak hydrogen bonding between a methine proton and oxygen atom (O31. . .H16 distance 2.55 Å) and possibly a weaker interaction with a methyl hydrogen (O32. . .H27A at 2.63 Å).

The H-bonding seems to be more limited in $Ln(NO_3)_3L_2$. There is a weak interaction between a methine proton in one molecule and O(10) on the nitrate of an adjacent molecule, which with an O. . .H distance of 2.586 Å is marginally shorter than the sum of Van der Waals radii.

The behaviour in CD_2Cl_2 solution has been investigated by variable temperature ^{31}P NMR spectroscopy and the data are collected in Table 5.

The spectra of the lighter lanthanides show very similar behaviour to those of other $Ln(NO_3)_3(R_3PO)_3$ complexes that we have previously analysed [12,13]. A strong temperature dependence is seen for the paramagnetic complexes with chemical shifts moving to high frequency with decreasing temperature for Ln = Ce–Sm and to low frequency for Eu–Yb. At low temperatures spectra readily assigned to static structures based on a pseudo *mer*-octahedron

Table 5
^{31}P NMR data for $Ln(NO_3)_3(^iPr_3PO)_n$ in CD_2Cl_2.

		Temperature (°C)			
Ln	*n*	20	−30	−60	−90
La	3	68.99[a]			68.94
Ce	3	109.7	119.5	128.9	143.2(2) 140.7(1)
Pr	3	161.2	193.6	228.7	331.0(2) 158.0(1)
Nd	3	169.00	193.6	223.3	296.2(2) 204.4(1)
Sm	3	66.18	69.74	72.96	77.52
Eu	3	−68.6	−90.7	−108.6	−137.8(2) −114.2(1)
Er	3	−123.6(2) −245.8(1)	−171.7(2) −310.2(1)		−316.7(2)[b] −356.8(1)[b] −198.2(2)[c] −220.8(1)[c]
Yb	2	−10.8	−31.3	−44.8	−52.8
Lu	2	72.2	70.7	70.6	70.8
Y	3	69.8	69.0[b]71.3[c]	68.9 $^2J_{PY}$ = 9.9 Hz[b] 70.7[c], 70.4[c]	68.8 $^2J_{PY}$ = 9.9 Hz[b] 71.0 $^2J_{PY}$ = 11.1 Hz[c] 70.4 $^2J_{PY}$ = 8.6 Hz[c] 69.8[c] 68.5 $^2J_{PY}$ = 9.8 Hz[c]
L		60.8			

[a] Ppm relative to external H_3PO_4.
[b] Major isomer.
[c] Minor isomer.

are seen for most complexes, where two signals in an approximately 2:1 ratio for the two different phosphorus environments are observed. A single peak at all temperatures was observed for the La and Sm complexes. In the case of La this indicates that there is rapid interchange between inequivalent environments on the NMR timescale even at −90 °C. The single signal seen for the Sm complex possibly arises from the small chemical shift difference between different environments. The observation of static structures as a function of the metal appears to correlate well with our earlier work, where the increasing steric demands/ligand basicity permit the observation of static structures for more of the metals. The overall pattern seems to be that static structures are favoured for smaller lanthanide ions and larger, more basic phosphine oxides.

The ^{31}P NMR spectra of the heavier lanthanide's complexes show the presence of more species in solution. The spectrum of the Er complex shows two peaks at ambient temperature in a 2:1 intensity ratio which are tentatively assigned to the two inequivalent phosphorus environments in the pseudo *mer*-octahedral geometry of the cation. At −90 °C a second pair of signals in a 2:1 ratio is also present and may be due to a small quantity of the neutral $Er(NO_3)_3L_3$ present in solution. The material isolated from the 1:3 $Lu(NO_3)_3$: $^{i}Pr_3PO$ reaction has more complex behaviour which is reminiscent in some respects to that of the complexes of Et_3PO with heavier lanthanides where the presence of $Ln(NO_3)_3L_3$ and $Ln(NO_3)_3L_2$ was deduced from elemental analyses and ^{31}P NMR spectra. Thus a single peak is observed in the ambient temperature spectrum as a result of rapid exchange between different complexes. The spectra show a single signal between 70.6 and 70.8 ppm which does not change between −30 and −90 °C assigned as $Lu(NO_3)_3L_2$. In addition many peaks which are tentatively assigned to a 2:1 compounds analogous to those formed with $^{t}Bu_3PO$ [14] and in solution by Et_3PO [13] are observable. Thus at −30 °C peaks at 72.7 and 65.4 ppm in a 2:1 ratio indicate the presence of a 1:3 complex. At lower temperature there are further changes to the ^{31}P NMR spectra, which show in addition to the strong signal at 70.6 from $Lu(NO_3)_3L_2$ additional peaks at 72.4, 71.6 with broad features at 73.3 and 67.2 ppm. This indicates that other processes are occurring, the nature of which at present is uncertain.

The ^{31}P NMR spectra of the isolated $Ln(NO_3)_3L_2$ Ln = Yb, Lu, show the single peak expected at all temperatures for a hexagonal bipyramidal structure analogous to those of $Ln(NO_3)_3(^{t}Bu_3PO)_2$.

3. Conclusion

The results show that with $^{i}Pr_3PO$ as ligand, lanthanide nitrate complexes form with two distinct stoichiometries in contrast to those formed with $^{i}Bu_3PO$ and Cy_3PO which form only $Ln(NO_3)_3L_3$ and $^{t}Bu_3PO$ which forms only $Ln(NO_3)_3L_2$. The system with $^{i}Pr_3PO$ allows the isolation of both 1:2 and 1:3 complexes for the first time in contrast to the related Et_3PO system in which mixtures were formed for the heavier lanthanides.

4. Experimental

Tri-isopropylphosphine oxide was prepared by oxidation of the phosphine with hydrogen peroxide. The phosphine (1.50 g, 9.36 mmol) was added to a solution of hydrogen peroxide in acetone (1.06 g 30% aqueous solution in 50 ml acetone). The temperature rose to 40 °C during the reaction. The mixture was stirred overnight and evaporated to give a colourless oil which was dried in vacuo over KOH (1.54 g, 93%).

NMR CD_2Cl_2 δ/ppm ^{31}P (161.8 MHz) 60.79 (s) ^{13}C (100.5 MHz) CH 24.64 (d) $^{1}J_{CP}$ = 61.5 Hz $CH_3$16.52 (d) $^{2}J_{CP}$ = 3.1 Hz ^{1}H (399.8 MHz) CH 2.102 (d, sept) $^{2}J_{HP}$ = 11.5 Hz, $^{3}J_{HH}$ = 7.3 Hz, CH_3 1.173 (d,d) $^{3}J_{HP}$ = 14.3 Hz, $^{3}J_{HH}$ = 7.3 Hz.

$La(NO_3)_3(^{i}Pr_3PO)_3$ $La(NO_3)_3{\cdot}7H_2O$ (0.16 g, 0.36 mmol) in 0.9 g ethanol was mixed with a solution of the ligand (0.20 g, 1.13 mmol) in 0.5 g ethanol. The solution was heated to 70 °C for 2 h, allowed to cool to room temperature and then stored at −30 °C overnight. The white crystals which formed were filtered, washed with cold ethanol and dried at the pump to give 0.23 g (75%).

Analysis% required (found) C 37.99 (37.74); H 7.44 (7.65); N 4.92 (5.00).

δ ^{31}P (161.8 MHz in CD_2Cl_2 at -90 °C) 68.94 ppm.

$Nd(NO_3)_3(^{i}Pr_3PO)_3$ $Nd(NO_3)_3{\cdot}6H_2O$ (0.16 g, 0.37 mmol) in 0.8 g ethanol was mixed with a solution of the ligand (0.21 g, 1.19 mmol) in 0.3 g ethanol. The solution was heated to 70 °C for 2 h, allowed to cool to room temperature and then stored at −30 °C for 5 d. The lilac powder which formed was filtered, washed with cold ethanol and dried at the pump to give 0.21 g (66%).

Analysis% required (found) C 37.75 (37.25); H 7.39 (7.25); N 4.89 (4.57).

δ ^{31}P (161.8 MHz in CD_2Cl_2 at −90 °C) 204.4 ppm (1), 296.2 ppm (2).

$Sm(NO_3)_3(^{i}Pr_3PO)_3$ $Sm(NO_3)_3{\cdot}6H_2O$ (0.18 g, 0.40 mmol) in 0.5 g ethanol was mixed with a solution of the ligand (0.19 g, 1.08 mmol) in 0.2 g ethanol. The solution was heated to 70 °C for 2 h, allowed to cool to room temperature and then stored at −30 °C for 5 d. The pale yellow powder which formed was filtered, washed with cold ethanol and dried at the pump to give 0.08 g (17%).

δ ^{31}P (161.8 MHz in CD_2Cl_2 at −90 °C) 77.52 ppm.

Analysis% required (found) C 37.49 (35.70); H 7.34 (7.02); N 4.85 (4.63).

$Eu(NO_3)_3(^{i}Pr_3PO)_3$ $Eu(NO_3)_3{\cdot}6H_2O$ (0.17 g, 0.38 mmol) in 0.9 g ethanol was mixed with a solution of the ligand (0.21 g, 1.19 mmol) in 0.3 g ethanol. The solution was heated to 70 °C for 2 h, allowed to cool to room temperature and then stored at −30 °C for 5 d. The colourless powder which formed was filtered, washed with cold ethanol and dried at the pump to give 0.18 g (55%).

Analysis% required (found) C 37.42 (37.21); H 7.33 (7.32); N 4.85 (4.47).

δ ^{31}P (161.8 MHz in CD_2Cl_2 at −90 °C) −114.2 ppm (1), −137.8 ppm (2).

$Er(NO_3)_3(^{i}Pr_3PO)_3[Er(NO_3)_3(^{i}Pr_3PO)_2]_2$;$Er(NO_3)_3{\cdot}6H_2O$ (0.18 g 0.39 mmol) in 0.8 g ethanol was mixed with a solution of the ligand (0.20 g mmol) in 0.5 g ethanol. The solution was heated to 70 °C for 2 h, allowed to cool to room temperature and then stored at −30 °C for 5 d. The pink powder which formed was filtered, washed with cold ethanol and dried at the pump to give 0.11 g (13%).

Analysis% required (found) C 32.99 (32.88); H 6.46 (6.41); N 5.55 (4.35).

δ ^{31}P (161.8 MHz in CD_2Cl_2 at −90 °C) major species −356.8 ppm (1), −316.7 ppm (2); minor species −220.8 ppm (1), −198.2 ppm (2).

$Yb(NO_3)_3(^{i}Pr_3PO)_2$;$Yb(NO_3)_3{\cdot}6H_2O$ (0.22 g 0.48 mmol) in 0.6 g ethanol was mixed with a solution of the ligand (0.16 g 0.89 mmol) in 0.4 g ethanol and heated to 70 °C for 2 h. Cooling the solution to −20 °C did not produce crystals. An equal volume of diethyl ether was layered on top of the ethanol solution and allowed to slowly diffuse at −20 °C. The crystals formed were filtered, washed with diethylether and dried at the pump to give 0.10 g (34%) white solid.

Analysis% required (found) C 30.38 (30.52); H 5.95 (6.02); N 5.90 (5.80).

δ ^{31}P (161.8 MHz in CD_2Cl_2 at −90 °C) −52.8 ppm.

$Lu(NO_3)_3(^iPr_3PO)_2$ $Lu(NO_3)_3 \cdot 6H_2O$ (0.10 g 0.20 mmol) in 0.3 g ethanol was mixed with a solution of the ligand (0.08 g 0.43 mmol) in 0.2 g ethanol and heated to 70 °C for 2 h. Cooling the solution to -20 °C did not produce crystals. An equal volume of diethyl ether was layered on top of the ethanol solution and allowed to slowly diffuse at −20 °C. The crystals formed were filtered, washed with diethylether and dried at the pump to give 0.03 g (21%) white solid.

Analysis% required (found) C 30.30 (30.29); H 5.93 (5.94); N 5.89 (5.70).

δ ^{31}P (161.8 MHz in CD_2Cl_2 at −90 °C) 70.8 ppm.

5. X-ray crystallography

Single-crystal X-ray diffraction analyses of **1**–**4** were performed at 120 K using a Bruker APEXII CCD diffractometer mounted at the window of a Bruker FR591 rotating anode (Mo Kα, λ = 0.71073 Å) and equipped with an Oxford Cryosystems Cryostream device. Data were processed using the COLLECT package [18].

The X-ray data for compounds **5** and **6** were collected at 100 K on Rigaku AFC12 goniometer equipped with an enhanced sensitivity (HG) Saturn 724+ detector mounted at the window of an FR−E + Superbright Mo Kα rotating anode generator with HF Varimax optics [19].

Unit cell parameters were refined against all data. An empirical absorption correction was carried out using SADABS [20] except compounds **5** and **6** for which CrystalClear [21] software was used.

All structures were solved by direct methods and refined on Fo^2 by full-matrix least-squares refinements using programs of the SHELX97 software [22]. All non-hydrogen atoms were refined with anisotropic displacement parameters. All hydrogen atoms were added at calculated positions and refined using a riding model with isotropic displacement parameters based on the equivalent isotropic displacement parameter (U_{eq}) of the parent atom.

Crystals of **4** were highly sensitive to solvent loss. Crystal structure of **4** contains infinitive channels of highly diffused solvent (EtOH) which was difficult to model correctly. SQUEEZE [23] routine of PLATON [24] was used to remove such diffused electron density from the crystal lattice. This resulted in better model and led structure refinement to convergence.

Crystal structures **5** and **6** are isostructural and contain two independent molecules. In both crystal structures all isopropyl groups are disordered and modelled over two sites. Four of them (two per each independent molecule) are disordered over symmetry element (mirror plane) and modelled in SHELXL with PART -1 command.

Furthermore, for disordered components vibrational restraints (SIMU/DELU), similar displacement restraints (EADP) and distance/angle restraints DFIX/DANG used to maintain sensible geometries and atomic displacement ellipsoids. Some atoms required ISOR restraint to approximate isotropic behaviour.

Additionally, crystal structure of **5** and **6** is merohedraly twinned and refined in SHELXL with applied twin law: 100 000 100 000 000 000 000 −100. Refined BASF = 0.07157 (~7% twinning) for **5** and 0.046 (~5% twinning) for **6**.

Figs. 1–3 were drawn in Olex2 [25], whereas Fig. 4 in Mercury [26].

Appendix A. Supplementary data

Crystallographic data (excluding structure factors) for the structures in this paper have been deposited with the Cambridge Crystallographic Data Centre, CCDC deposition numbers 949790–949795 contains the supplementary crystallographic data for this paper. This data can be obtained free of charge from The Cambridge Crystallographic Data Centre via www.ccdc.cam.ac.uk/data_request/cif. Supplementary data associated with this article can be found, in the online version, at http://dx.doi.org/10.1016/j.poly.2013.10.028.

References

[1] W. Levason, E.H. Newman, M. Webster, Acta Crystallogr., Sect. C56 (2000) 1308.
[2] W. Levason, E.H. Newman, M. Webster, Polyhedron 19 (2000) 2697.
[3] M.J. Glazier, W. Levason, M.L. Matthews, P.L. Thornton, M. Webster, Inorg. Chim. Acta 357 (2004) 1083.
[4] A. Bowden, A.W.G. Platt, K. Singh, R. Townsend, Inorg. Chim. Acta 363 (2010) 243.
[5] A.M.G. Massabni, N.L.R. Gibran, O.A. Serra, Inorg. Nucl. Chem. Lett. 14 (1978) 419.
[6] V.K. Manchanda, K. Chander, N.P. Singh, G.M. Nair, J. Inorg. Nucl. Chem. 39 (1977) 1039.
[7] J. Goffart, G. Duyckaerts, Anal. Chim. Acta 46 (1969) 91.
[8] W. Jianchen, S. Chongli, Solvent Extr. Ion Exch. 19 (2001) 231.
[9] W.D. Euan, P. Cao, Y. Zhu, J. Rare Earths 28 (2010) 211.
[10] M.L.P. Reddy, J.R. Bosco Bharathi, S. Peter, T.R. Ramamohan, Talanta 50 (1999) 79.
[11] A.P. Hunter, A.M.J. Lees, A.W.G. Platt, Polyhedron 26 (2007) 4865.
[12] A. Bowden, P.N. Horton, A.W.G. Platt, Inorg. Chem. 50 (2011) 2553.
[13] A. Bowden, K. Singh, A.W.G. Platt, Polyhedron 42 (2012) 30.
[14] A. Bowden, S.J. Coles, M.B. Pitak, A.W.G. Platt, Inorg. Chem. 51 (2012) 4379.
[15] J.C. Bollinger, R. Houriet, C.W. Kern, D. Perret, J. Weber, T. Yvernault, J. Am. Chem. Soc. 107 (1985) 5352.
[16] C.A. Tolman, Chem. Rev. 77 (1977) 345.
[17] M. Bosson, W. Levason, T. Patel, M.C. Popham, M. Webster, Polyhedron 20 (2001) 2055.
[18] R. Hooft, Collect: Data Collection Software; B.V. Nonius: Delft: Netherlands, 1998.
[19] S.J. Coles, P.A. Gale, Chem. Sci. 3 (2012) 683.
[20] G.M. Sheldrick, SADABS, Version 2.10, Bruker AXS Inc., Madison, Wisconsin, USA, 2003.
[21] CrystalClear-SM Expert 3.1 b26 (Rigaku, 20112).
[22] G.M. Sheldrick, SHELXL97, Acta Crystallogr., Sect. A64 (2008) 112.
[23] P. van der Sluis, A.L. Spek, Acta Crystallogr., Sect. A46 (1990) 194.
[24] A.L. Spek, J. Appl. Cryst. 36 (2003) 7.
[25] C.F. Macrae, I.J. Bruno, J.A. Chisholm, P.R. Edgington, P. McCabe, E. Pidcock, L. Rodriguez-Monge, R. Taylor, J. van de Streek, P.A. Wood, Mercury CSD 2.0 – new features for the visualization and investigation of crystal structures, J. Appl. Cryst. 41 (2008) 466.
[26] O.V. Dolomanov, L.J. Bourhis, R.J. Gildea, J.A.K. Howard, H. Puschmann, OLEX2: a complete structure solution, refinement and analysis program, J. Appl. Cryst. 42 (2009) 339.